JOC Article

Aromaticity and Homoaromaticity in Methano[10]annulenes

Giovanni F. Caramori,[†] Kleber T. de Oliveira,[†] Sérgio E. Galembeck,*[,†] Patrick Bultinck,[‡] and Mauricio G. Constantino[†]

Departamento de Química, FFCLRP, Universidade de São Paulo, 14040-901, Ribeirão Preto − SP, Brazil, and Department of Inorganic and Physical Chemistry, Ghent University, Krijgslaan 281 (S3), B-9000 Gent, Belgium

segalemb@usp.br

Received August 16, 2006

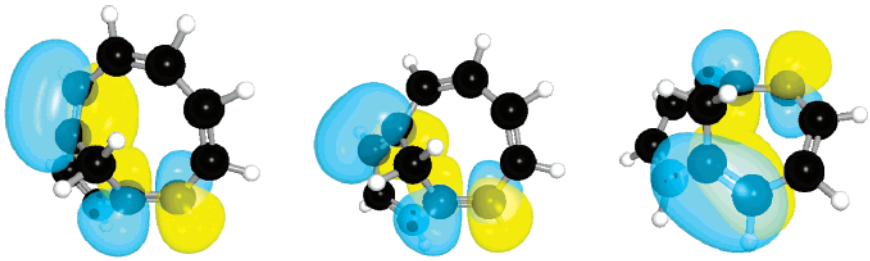

Aromaticity and neutral homoaromaticity have been evaluated in methano[10]annulenes systems, 1,4-methano[10]annulene (**1**), 1,5-methano[10]annulene (**2**), and 1,6-methano[10]annulene (**3**). C−C bond lengths indicate that **1** presents higher bond alternation than **2** and **3**. The relative energies were determined at the B3LYP/6-311+G(d,p) level, and they pointed out that **3** is the most stable isomer. Strain energies, evaluated employing homodesmotic reactions, show the same order as the relative energies. Through a decomposition of strain energies, it could be concluded that the rings absorb more tension than the bridges. The changes in aromaticity were evaluated by magnetic susceptibilities, χ_M, HOMA, NICS, and resonance energies, RE. HOMA, RE, and χ_M indicate that **2** and **3** are strongly, and **1** is fairly, aromatic. NICS does not provide reliable results, due to interference of ring and bridge atoms. NBO analysis presents some interactions that suggest the existence of neutral homoaromaticity. GPA indices (evaluated at the B3LYP/6-31G* level) point out that homoaromaticity plays a relevant role only in **3**. Moreover, this work is the first in the current literature that studies 1,4-methano[10]annulene (**1**).

1. Introduction

Since the original preparation of the parent 1,6-methano[10]-annulene (**3**), by Vogel and Roth,[1] bridged annulenes have been the subject of numerous synthetic investigations.[2] These compounds have presented some important applications; for example, derivatives of **3** have been applied in biological studies due to their structural properties, allowing the evaluation of effects of amphiphilic topology on self-association in solution.[3] In general, the bridged methano[10]annulenes constitute a very interesting class of compounds to investigate aromaticity because experimental analyses such as NMR[4] and chemical reactivity have confirmed the aromatic nature of these compounds. For example, some derivatives of 1,6-methano[10]annulene (**3**) can stabilize carbocations[5] and radicals with similar stability of benzylic radicals.[6] In addition, the 1,5-methano[10]annulene (**2**) undergoes Friedel−Crafts reactions, and its heats of hydrogenation reveal that the parent hydrocarbon undergoes an aromatic stabilization.[7]

* Corresponding author. Phone: (+55)-16-3602-37-65. Fax: (+55)-16-3602-48-38.
[†] Universidade de São Paulo.
[‡] Ghent University.

(1) (a) Vogel, E.; Roth, H. D. *Angew. Chem.* **1964**, *76*, 145. (b) Vogel, E. *Chimia* **1968**, *22*, 21.
(2) (a) Vogel, E.; Schröck, W.; Böll, W. A. *Angew. Chem., Int. Ed. Engl.* **1966**, *5*, 732. (b) Scott, L.; Brunsvold, W. R. *J. Am. Chem. Soc.* **1978**, *100*, 4320. (c) Barrett, D. G.; Liang, G. B.; Gellman, S. H. *J. Am. Chem. Soc.* **1992**, *114*, 6915. (d) Barrett, D. G.; Liang, G. B.; McQuade, D. T.; Desper, J. M.; Schladtzky, K. D.; Gellman, S. H. *J. Am. Chem. Soc.* **1994**, *116*, 10525. (e) Rigby, J. H.; Saha, A.; Heeg, M. J. *J. Org. Chem.* **1997**, *62*, 6448. (f) Kuroda, S.; Oda, M.; Zuo, S.; Kanayama, S.; Shah, S. I. M.; Furuta, S.; Miyatake, R.; Kyogoku, M. *Tetrahedron Lett.* **2001**, *42*, 6345.
(3) Barrett, D. G.; Gellman, S. H. *J. Am. Chem. Soc.* **1993**, *115*, 9343.
(4) Mitchell, R. H. *Chem. Rev.* **2001**, *101*, 1301−1315.
(5) Creary, X.; Miller, K. *J. Org. Chem.* **2003**, *68*, 8683.
(6) Creary, X.; Miller, K. K. *Org. Lett.* **2002**, *4*, 3493.

10.1021/jo061702v CCC: $37.00
Published on Web 12/07/2006

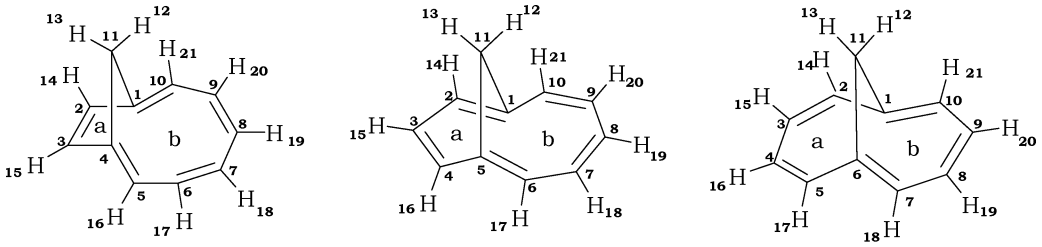

1 **2** **3**

FIGURE 1. The methano[10]annulenes.

The first theoretical studies about methano-bridged annulenes date from the 1970s. A remarkable work was realized by Gavezzoti and Simonetta, which reports results of stability, aromaticity, and reactivity of the bridged [10]-, [12]-, and [14]-annulenes, obtained through extended Hückel molecular orbital calculations.[8] Another study, reported by Grunewald et al., describes an extensive investigation to explore the reactivity and aromaticity of the 1,6-methano[10]annulene (**3**), and naphthalene (**4**), by using ab initio and semiempirical methods.[9] They compared the aromaticity of **3** and **4** through the average π-electron energy per π-electron pair as a measure of aromaticity, and they pointed out that **3** presents an aromaticity similar to **4**.[9] Espinosa-Müller and Meezes had also related the relative strain energy of **2** and **3** by using molecular mechanics methods, and they concluded that **3** was 20.88 kcal mol^{-1} more stable than **2**.[10] Many other theoretical studies about the bridged[10]-annulenes, reported on the current literature, have generally been computed at ab initio[11] or valence bond theory[12] levels of theory. For instance, Haddon and Raghavachari compared the relative stabilities of **2** and **3**, through HF and MPn methods, concluding that **3** is 15.6 kcal mol^{-1} more stable than **2**.[13] Other papers have calculated geometrical parameters and spectroscopic data, which presented close agreement with the X-ray diffraction, infrared, and Raman spectroscopy data.[14] Jiao and co-workers explored how the stability and the aromaticity (through the NICS criterion) of the 1,6-X-[10]annulenes, (X = SiH_2, $SiMe_2$, PH, CH_2, NH, O, and S) are affected by the substitution at the bridges. They also showed that 1,6-X-[10]annulenes, substituted with X = SiH_2, $SiMe_2$, PH, and S, presented the largest strain energies.[15] Despite the above-mentioned citations, theoretical studies that explore the aromaticity or the homoaromaticity of methano[10]annulenes by using current computational methods are not found in the literature, especially to understand the properties of the hypothetical 1,4-methano[10]annulene (**1**).

Homoaromaticity, the presence of aromaticity despite an interruption in the formal cyclic conjugation, has been verified theoretically and experimentally for cations.[16] However, neutral homoaromaticity is a matter of strong debate, and several authors do not believe in its existence.[16] In recent years, theoretical evidence indicates that neutral compounds can be homoaromatic. Some boron analogues of 1,3-dehydro-5-adamantyl were studied, and geometries and chemical shifts indicated that homoconjugation is present in these systems.[17] Several spherical sila- and germa-homoaromatic compounds and clusters were designed, and they present strong electron delocalization.[18] The homoaromaticity of semibullvalenes was strongly debated, but Borden et al. indicate that some substituents can stabilize the bishomoaromatic form.[19] The tris-homoaromaticity was studied for tris(bismethano)benzene and some derivatives using magnetic, energetic, and geometric properties. It was concluded that this compound and one other derivative are homoaromatic.[20] The electron localization function has been used to determine the homoaromaticity of some carbo[*N*]annulenes and [*N*]-pericyclynes. Only one neutral molecule is homoaromatic.[21] Some bicyclo[3.2.1]octane derivatives were investigated, and the results indicate that some of them are homoaromatic, others are nonhomoaromatic, and some others are antihomoaromatic.[22,27]

The purpose of this paper is to study the electronic structure, the aromaticity, and neutral homoaromaticity of the bridged methano[10]annulenes **1**, **2**, and **3** (Figure 1), by using DFT calculations and natural bond orbital (NBO),[23] natural resonance theory (NRT),[24] natural steric analysis (NSA),[25] atoms in molecules (AIM)[26] methods, and generalized population analysis (GPA).[27] The strain energies were calculated by homodesmotic reactions, and aromaticity was evaluated by magnetic susceptibilities,[28] HOMA (harmonic oscillator measure of aromatic-

(7) Scott, L. T.; Sumpter, C. A.; Gantzel, P. K.; Maverick, E.; Trueblood, K. N. *Tetrahedron* **2001**, *57*, 3795.
(8) Gavezzotti, A.; Simonetta, M. *Helv. Chim. Acta* **1976**, *59*, 2984.
(9) Grunewald, G. L.; Uwaydah, I. M.; Christoffersen, R. E.; Spangler, D. *Tetrahedron Lett.* **1975**, *11*, 933.
(10) Espinosa-Müller, A.; Meezes, F. C. *J. Chem. Phys.* **1978**, *69*, 367−372.
(11) (a) Farnell, L.; Radom, L. *J. Am. Chem. Soc.* **1982**, *104*, 7650. (b) Gatti, C.; Barzaghi, M.; Simonetta, M. *J. Am. Chem. Soc.* **1985**, *107*, 878. (c) Simonetta, M.; Barzaghi, M.; Gatti, C. *J. Mol. Struct. (THEOCHEM)* **1986**, *138*, 39. (d) Bock, C. W.; George, P.; Gluster, J. P. *J. Mol. Struct. (THEOCHEM)* **1991**, *234*, 227. (e) George, P.; Clusker, J. P.; Bock, C. W. *J. Mol. Struct. (THEOCHEM)* **1991**, *235*, 193.
(12) Sironi, M.; Raimondi, M.; Copper, D. L.; Gerratt, J. *J. Mol. Struct. (THEOCHEM)* **1995**, *338*, 257.
(13) Haddon, R. C.; Raghavachari, K. *J. Am. Chem. Soc.* **1985**, *107*, 289.
(14) Gellini, C.; Salvi, P. R.; Vogel, E. *J. Phys. Chem. A* **2000**, *104*, 3110.
(15) Jiao, H.; van Eikema Hommes, N. J. R.; Schleyer, P. v. R. *Org. Lett.* **2002**, *4*, 2393.
(16) Williams, R. V. *Chem. Rev.* **2001**, *101*, 1185.
(17) Olah, G. A.; Rasul, G.; Prakash, G. K. S. *J. Org. Chem.* **2000**, *65*, 5956.
(18) Chen, Z.; Hirsch, A.; Nagase, S.; Thiel, W.; Schleyer, P. v. R. *J. Am. Chem. Soc.* **2003**, *125*, 15507.
(19) Brown, E. C.; Henze, D. K.; Borden, W. T. *J. Am. Chem. Soc.* **2002**, *124*, 14977.
(20) Stahl, F.; Schleyer, P. v. R.; Jiao, H.; Schaefer, H. F.; Chen, K. H.; Allinger, N. L. *J. Org. Chem.* **2002**, *67*, 6599.
(21) Lepetit, C.; Silvi, B.; Chauvin, R. *J. Phys. Chem. A* **2003**, *107*, 464.
(22) Freeman, P. K. *J. Org. Chem.* **2005**, *70*, 1998.
(23) Carpenter, J. E.; Weinhold, F. *J. Mol. Struct. (THEOCHEM)* **1988**, *169*, 41.
(24) (a) Glendening, E. D.; Weinhold, F. *J. Comput. Chem.* **1998**, *19*, 593. (b) Glendening, E. D.; Weinhold, F. *J. Comput. Chem.* **1998**, *19*, 610.

TABLE 1. Geometrical Parameters of 1, 2, and 3

geometrical parameters	compounds 1	2	3	3(exp)[39]
	Bond Distances (Å)			
C(2)−C(3)	1.383	1.412	1.392	1.376
C(3)−C(4)	1.446	1.412	1.424	1.418
C(4)−C(5)	1.358	1.403	1.392	1.373
C(4)−C(11)	1.499			
C(5)−C(6)	1.441	1.392	1.409	1.405
C(5)−C(11)		1.497		
C(6)−C(7)	1.389	1.406	1.409	1.403
C(6)−C(11)			1.492	1.487
C(7)−C(8)	1.456	1.415	1.392	1.379
C(1)−C(4)	2.274			
C(1)−C(5)		2.376		
C(1)−C(6)			2.278	
	Bond Angles (deg)			
C(1)C(11)C(4)	98.6			
C(1)C(11)C(5)		105.0		
C(1)C(11)C(6)			99.6	97.6
C(2)C(3)C(4)	108.0	121.3	127.7	127.6
C(3)C(4)C(5)	130.0	117.0	127.7	127.1
C(4)C(5)C(6)	123.2	128.7	122.5	123.1
C(5)C(6)C(7)	135.0	123.7	126.5	126.8
C(6)C(7)C(8)	142.7	133.9	122.5	122.8
	Dihedral Angles (deg)			
C(1)C(2)C(3)C(4)	0.0	−12.7	−19.2	
C(1)C(11)C(4)C(3)	−37.7			
C(1)C(11)C(5)C(4)		−61.0		
C(1)C(11)C(6)C(5)			−86.1	
C(2)C(3)C(4)C(5)	−129.0			
C(3)C(4)C(5)C(6)	139.7	−137.6	19.2	
C(4)C(5)C(6)C(7)	−25.2	142.1	−144.6	
C(5)C(6)C(7)C(8)	−5.0	−17.2	144.6	
C(6)C(7)C(8)C(9)	−0.1	−8.7	−19.2	

ity),[29] NICS (nucleus independent chemical shift),[30] and resonance energies (RE).[31]

2. Computational Methods

The geometries of all molecules were fully optimized. The Hessian showed that all optimized geometries are minima. The aromaticity was calculated by the magnetic susceptibility,[28] NICS,[30] HOMA,[29] and RE, which was determined through the HOMO−LUMO gap.[31] All of these calculations were done at the B3LYP/6-311+G(d,p)[32,33] level in Gaussian 98.[34] NICS was calculated by GIAO,[35] and magnetic susceptibilities were calculated by CSGT.[36] Wavefunction analysis was performed via NBO,[23] NSA,[25] and NRT[24] methods. These calculations were done with the NBO 5.0 program[37] interfaced with Gaussian 98. The AIM analyses of electron density were performed with AIM2000.[38] GPA measures were computed using B3LYP/6-31G* geometries and density matrices for all molecules, employing self-developed software.

TABLE 2. ZPE Corrected Total Energies (*E*+ZPE), and Relative Energies Δ*E*

compounds	*E*+ZPE (hartree)	Δ*E* (kcal mol^{-1})
1	−424.997006	40.44
2	−425.035037	16.58
3	−425.061458	0.00

TABLE 3. Strain Energies of 1−3 (kcal mol^{-1})

Homodesmotic Reactions	SE(HD)
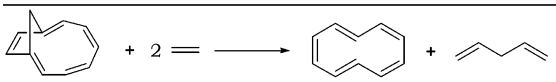	-13.84
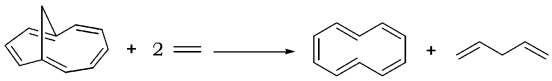	10.02
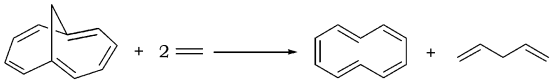	26.60

TABLE 4. Partitioning of Strain Energies (kcal mol^{-1})

compounds	SE(ba)	SE(br)	SE(sum)	SE(rep)	SE(ba)/SE(sum)
1	55.72	14.98	70.70	84.54	0.79
2	36.33	8.32	44.65	34.63	0.81
3	11.09	16.11	27.27	0.61	0.41

3. Results and Discussion

3.1. Molecular Structure. The calculations indicate that **1**, **2**, and **3** belong to the C_s, C_s, and C_{2v} point groups, respectively. Table 1 presents the geometries for all methano[10]annulenes. It can be observed that the geometry of **3** is in close agreement with the experimental values, obtained through X-ray diffraction.[39] **1** presents a larger alternation in carbon−carbon bond lengths as compared to **2** and **3**, indicating smaller resonance for the former. In contrast, the bond lengths of methano bridges are fairly constant for all compounds. The CCC bond angles in the ring are around the sp^2 value for **3**. Compound **2** presents some angles around the bridgehead carbon with values larger

(25) (a) Badenhoop, J. K.; Weinhold, F. *J. Chem. Phys*. **1997**, *107*, 5406. (b) Badenhoop, J. K.; Weinhold, F. *J. Chem. Phys*. **1997**, *107*, 5422.
(26) Bader, R. F. W. *Atoms in Molecules, A Quantum Theory*; Claredon Press - Oxford: Oxford, 1994.
(27) Ponec, R.; Bultinck, P.; Saliner, A. G. *J. Phys. Chem. A* **2005**, *109*, 6606.
(28) (a) Chen, Z.; Wannere, C. S.; Corminboeuf, C.; Puchta, R.; Schleyer, P. v. R. *Chem. Rev.* **2005**, *105*, 3842. (b) Gomes, J. A. N. F.; Mallion, R. B. *Chem. Rev.* **2001**, *101*, 1349.
(29) Krygowski, T. M.; Cyrañski, M. K.; Czarnocki, Z.; Häfelinger, G.; Katritzky, A. R. *Tetrahedron* **2000**, *56*, 1783.
(30) Schleyer, P. v. R.; Maerker, C.; Dransfeld, A.; Jiao, H.; van Eikema Hommes, N. J. R. *J. Am. Chem. Soc.* **1996**, *118*, 6317.
(31) Proft, F. D.; Geerlings, P. *Chem. Rev.* **2001**, *101*, 1451.
(32) Becke, A. D. *J. Chem. Phys.* **1993**, *98*, 5648.
(33) Curtiss, L. A.; McGrath, M. P.; Blaudeau, J. P.; Davis, N. E.; Binning, R. C., Jr.; Random, L. *J. Chem. Phys.* **1995**, *103*, 6104.
(34) Frisch, M. J.; Trucks, G. W.; Schlegel, H. B.; Scuseria, G. E.; Robb, M. A.; Cheeseman, J. R.; Zakrzewski, V. G.; Montgomery, J. A.; Stratmann, R. E.; Burant, J. C.; Dapprich, S.; Millam, J. M.; Daniels, A. D.; Kudin, K. N.; Strain, M. C.; Farkas, O.; Tomasi, J.; Barone, V.; Cossi, M.; Cammi, R.; Mennucci, B.; Pomelli, C.; Adamo, C.; Clifford, S.; Ochterski, J.; Petersson, G. A.; Ayala, P. Y.; Cui, Q.; Morokuma, K.; Malick, D. K.; Rabuck, A. D.; Raghavachari, K.; Foresman, J. B.; Cioslowski, J.; Ortiz, J. V.; Stefanov, B. B.; Liu, G.; Liashenko, A.; Piskorz, P.; Komaromi, I.; Gomperts, R.; Martin, R. L.; Fox, D. J.; Keith, T.; Al-Laham, M. A.; Peng, C. Y.; Nanayakkara, A.; Gonzalez, C.; Challacombe, M.; Gill, P. M. W.; Johnson, B. G.; Chen, W.; Wong, M. W.; Andres, J. L.; Head-Gordon, M.; Replogle, E. S.; Pople, J. A. *Gaussian 98*, revision A.7; Gaussian, Inc.: Pittsburgh, PA, 1998.
(35) Ditchfield, R. *Mol. Phys.* **1974**, *27*, 789.
(36) Cheeseman, J. R.; Frisch, M. J.; Trucks, G. W.; Keith, T. A. *J. Chem. Phys.* **1996**, *104*, 5497.
(37) NBO 5.0: Glendening, E. D.; Badenhoop, J. K.; Reed, A. E.; Carpenter, J. E.; Bohmann, J. A.; Morales, C. M.; Weinhold, F. Theoretical Chemistry Institute, University of Wisconsin, Madison, WI, 2001.
(38) AIM2000, Version 2.0, Copyright Program designed by Friedrich Biegler-König and Jens Schönbohm; Chemical advice by R. F. W. Bader, McMaster University, Hamilton, Canada, 2002.
(39) Bianchi, R.; Pilati, T.; Simonetta, M. *Acta. Crystallogr.* **1980**, *B36*, 3146.

TABLE 5. HOMA, EN, and GEO of Compounds 1−4

	ring (a)			ring (b)			global		
	HOMA	EN	GEO	HOMA	EN	GEO	HOMA	EN	GEO
1	0.410	0.359	0.231	0.554	0.070	0.376	0.511	0.133	0.356
2	0.897	0.098	0.005	0.905	0.070	0.025	0.901	0.081	0.018
3	0.886	0.076	0.038	0.886	0.076	0.038	0.886	0.076	0.038
4	0.783	0.082	0.135	0.783	0.082	0.135	0.783	0.082	0.135

TABLE 6. Magnetic Susceptibilities for 1−3 (cgs ppm)

compounds	$-\chi_M$
1	95.9
2	109.7
3	111.4

than 120°, indicating some tension in ring (b) of the bicyclo (Figure 1). The tension, as indicated by the bond angles, is larger for **1**, because this compound presents a four- and an eight-membered ring. This suggests that the sterically most stable compound is **3** and the least is **1**. The planarity of the annulenes **1**, **2**, and **3** was estimated through the dihedral angles in the neighborhood of the methano bridges. Comparing these angles, C(2)C(3)C(4)C(5) and C(3)C(4)C(5)C(6) for **1**, C(3)C(4)C(5)C(6) and C(4)C(5)C(6)C(7) for **2**, and C(4)C(5)C(6)C(7) and C(5)C(6)C(7)C(8) for **3**, it can be concluded that the order of planarity is **3** > **2** > **1**, with the largest variation from **1** to **2**. As planarity is typical for high aromaticity, it is also probable that the aromaticity follows the same stability order.

3.2. Energies. The relative energies indicate that **1** is the least stable isomer, **2** presents an intermediate stability, and **3** is the most stable (Table 2). The large differences in the relative energies can be attributed to the strain differences, which are caused by the methano bridges and by the bent rings. A deeper understanding of the strain energies was obtained by the analysis of the tensions of the methano bridges and the rings by using homodesmotic reactions.

3.3. Homodesmotic Reactions. Homodesmotic reactions are widely used to evaluate tension in cyclic organic compounds.[40] The strain energies obtained through these reactions, SE(HD) (Table 3), indicate that **1** is the most strained, **2** presents an intermediate tension, and **3**, which presents a large aromatic stabilization, according to the HOMA values (next section), is the least strained isomer. Relative energies follow the same order as the homodesmotic reactions, indicating that the interactions between methano bridges and rings and the bending on the rings are the two main factors that control the stability of these compounds.

To separate the deformations on the bond lengths and nonbonded interactions that affect SE(HD), a partitioned treatment of the strain energies was considered (Table 4).[41] In this approach, the bridges of the methano[10]annulenes **1**−**3** were disconnected, while the structure of the [10]annulene was maintained in the original geometry. The free valencies of both rings and bridges were saturated with hydrogen atoms. Separate single-point calculations were performed on both the [10]-annulene and the bridges, maintaining both in the original conformations of the corresponding methano[10]annulenes **1**−**3**. The obtained values were compared with the energy of the optimized reference compounds, [10]annulene and propane. These differences provided the steric energies of the bent annulenes, SE(ba), and of the bridges, SE(br). The sum of these components is designated SE(sum). According to Table 4, the SE(ba) values of **1** and **2** indicate that the rings of these isomers absorb more strain than the methano bridges. On the other hand, the annulene **3** presents the smallest values of SE(ba) and the largest values of SE(br), and in this case the methano bridge absorbs more tension than the ring. The total strain energy, SE-(sum), is largely determined by the annulene component, and SE(ba) differs by a factor 5 between **3** and **1**. In contrast, the most tensioned bridges are **3** and **1** and the least is **2**, and the range of values of SE(br) is substantially smaller. This can be explained by the small variations in bridged bond lengths and bond angles and by the less strained bridged bond angle for **2** (Table 1). The repulsive nature of the interactions between rings and bridges is computed by the component SE(rep), which is the difference between SE(sum) and SE(HD). Considering the obtained values of SE(rep), we note that the same trend is observed for SE(ba) and SE(sum) and for SE(HD) and ΔE. This indicates that the relative stability is largely determined by the annulene strain and by the repulsion between the bridge and the annulene. The coefficient SE(ba)/SE(sum) provides additional information about the distribution of SE. According to the SE(ba)/SE(sum) values, the rings of **1** and **2** support more

TABLE 7. NICS (ppm) for Compounds 1−4

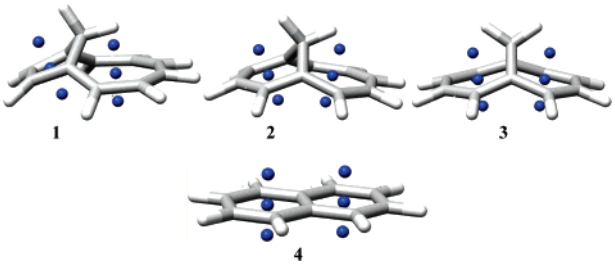

	ring (a)			ring (b)		
compounds[a]	NICS(−1)	NICS(0)	NICS(1)	NICS(−1)	NICS(0)	NICS(1)
1	−19.3	−17.1	−8.4	−16.4	−7.7	−14.5
2	−19.5	−17.9	−9.7	−14.3	−12.8	−12.0
3	−16.4	−14.8	−10.3	−16.4	−14.8	−10.3
4	−10.7	−8.6	−10.7	−10.7	−8.6	−10.7

[a] Reference compound: benzene, NICS(0) = −8.41 ppm, NICS(1) = −10.4 ppm.

TABLE 8. Resonance Energy, HOMO−LUMO Gap (kcal/mol), and Bond Orders

compounds	RE	ΔE_g	P_{rs}
1	72.32	−84.34	1.444
2	79.40	−87.55	1.485
3	88.39	−102.23	1.450
4	95.62	−109.49	1.457

(40) George, P.; Glusker, J. P.; Charles, C. W. *J. Mol. Struct. (THEOCHEM)* **1991**, *235*, 193.

(41) van Eis, M. J.; Wolf, W. H.; Bickelhaupt, F.; Boese, R. *J. Chem. Soc., Perkin Trans. 2* **2000**, 793.

TABLE 9. Resonance Structures, Degeneracy (deg), and Weights

Compounds	Structure	deg	Weight (%)
1	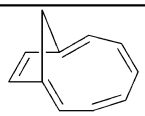	1	44.3
	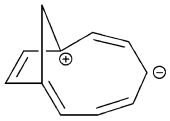	1	11.0
2	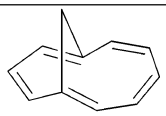	2	42.7
3	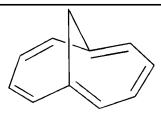	2	24.5
4	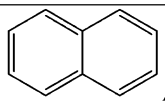 A	2	33.6
	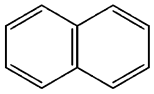 B	1	25.5

TABLE 10. Second-Order Stabilization Energy, $\Delta E^{(2)}$, for the Main Resonance Structures

	$\Delta E^{(2)}$ (kcal/mol)		
interactions	**1**	**2**	**3**
$\pi_{C(1)-C(2)} \rightarrow \pi^*_{C(3)-C(4)}$		23.45	
$\pi_{C(2)-C(3)} \rightarrow \pi^*_{C(4)-C(5)}$	17.12		18.20
$\pi_{C(3)-C(4)} \rightarrow \pi^*_{C(5)-C(6)}$		22.42	
$\pi_{C(4)-C(5)} \rightarrow \pi^*_{C(6)-C(7)}$	15.21		17.30
$\pi_{C(5)-C(6)} \rightarrow \pi^*_{C(7)-C(8)}$		20.47	
$\pi_{C(6)-C(7)} \rightarrow \pi^*_{C(8)-C(9)}$	15.01		23.69
$\pi_{C(7)-C(8)} \rightarrow \pi^*_{C(9)-C(10)}$		18.56	
$\pi_{C(8)-C(9)} \rightarrow \pi^*_{C(1)-C(10)}$	11.62		20.15
$\pi_{C(9)-C(10)} \rightarrow \pi^*_{C(1)-C(2)}$		19.64	
$\pi_{C(10)-C(1)} \rightarrow \pi^*_{C(2)-C(3)}$	13.46		17.73

tension than the ring of **3**. The obtained results, except for **3**, present a close agreement with those observed for [2.2]-cyclophanes, which suggest that the rings can absorb more tension than the bridges.[42]

3.4. Aromaticity. Because aromaticity is a multidimensional phenomenon, this section presents four different aromatic criteria, the geometric HOMA (harmonic oscillator model of aromaticity), the magnetic susceptibility, NICS (nucleus independent chemical shift), and the energetic RE (resonance energy), obtained through the HOMO−LUMO gap.

3.4.1. HOMA. The HOMA criterion was applied to compounds **1**−**3** and to naphthalene (**4**), to investigate the effects of geometry on the aromaticity (Table 5). HOMA was evaluated not only for the whole molecule but also for the individual rings (a) and (b) (Figure 1).

(42) Caramori, G. F.; Galembeck, S. E.; Laali, K. K. *J. Org. Chem.* **2005**, *70*, 3242.

TABLE 11. Second-Order Stabilization Energy, $\Delta E^{(2)}$, Energy Splitting of Donor and Acceptor Orbitals, $\epsilon_i - \epsilon_j$, and the Element of the Fock Matrix, $F(i,j)$

compounds	interactions	$\Delta E^{(2)}$ (kcal/mol)	$\epsilon_i - \epsilon_j$ (au)	$F(i,j)$ (au)
1	$\pi_{C(1)-C(10)} \rightarrow \pi^*_{C(4)-C(5)}$	0.52	0.31	0.011
2	$\pi_{C(1)-C(2)} \rightarrow \pi^*_{C(5)-C(6)}$	1.40	0.28	0.016
3	$\pi_{C(6)-C(7)} \rightarrow \pi^*_{C(1)-C(10)}$	3.40	0.27	0.027

Global HOMA indicates that **2** and **3** have a high aromaticity, larger than **4**, and **1** is fairly aromatic. The main factor that contributes to the low aromaticity of **1** is the alternation of C−C bonds, or GEO, as reported above (Table 1). GEO, or the geometric component of HOMA, is also the main factor for the not so high aromaticity of **4** and also determines the HOMA global order of aromaticity. In contrast, the small reduction of the aromaticity of **2** and **3** is due to C−C bond elongation or shrinking from the standard value, EN, or the energetic component of HOMA. An analysis of (a) and (b) for **1** indicates that the eight-membered ring, (b), presents a higher aromaticity than the four-membered one, (a), due to a larger reduction of EN term, despite the increase of GEO. In addition, HOMAs of the individual rings of **2** are quite similar, despite different sizes.

3.4.2. Magnetic Susceptibility. The increased diamagnetic susceptibility, χ_M, was widely used to analyze the global aromatic character.[28] Aromatic compounds present significantly exalted χ_M and high anisotropy. The first is normally obtained by a comparison between the bulk magnetic susceptibility and χ_M obtained by bond and atom increments, or it needs a suitable reference. This criterion is the only one that is uniquely associated with aromaticity, as stated by Schleyer and Gao.[43] The latter is only applicable to planar compounds. To overcome the choice of appropriate reference systems, and considering that **1**−**3** are isomers, a direct comparison of χ_M was made. A similar approach was used in the study of large [*N*]phenylenes.[44] Table 6 indicates that **1** is much less aromatic than **2** and **3**, as was observed in global HOMA (Table 5). For both global indexes, the aromaticities of **2** and **3** are almost equal.

3.4.3. NICS. The magnetic criterion of aromaticity NICS was applied to compounds **1**−**3**. In addition, the same analysis was extended to naphthalene **4**. To avoid confusion, the notation NICS(distance, ring fragment) was adopted. For example, NICS-(1,a) refers to the NICS calculated 1 Å above the plane of the ring fragment (a). The positive direction is defined as the side where the bridge is located.

NICS analysis was first tested for **4** (Table 7). NICS values indicate that **4** is as aromatic as benzene.[16] The use of NICS for the quantification of benzene like aromaticity in polycyclic molecules is, however, debated.[45b] For **1** and **2**, some NICS values are very high, as NICS(−1) for both rings and NICS(1) for ring (b), indicating that these compounds have a high aromaticity. The order of aromaticity for a ring measured 1 Å in the positive direction or in the negative direction presented discrepant results and does not agree with HOMA or with the strain energies, SE(HD) or SE(ba) (Tables 3 and 4). These discrepancies indicate that the applicability of NICS for methano-bridged annulenes is limited. They can be attributed

(43) Schleyer, P. v. R.; Gao, H. *Pure Appl. Chem.* **1996**, *68*, 209.
(44) Schulman, J. M.; Disch, R. L. *J. Phys. Chem. A* **2003**, *107*, 5223.
(45) (a) Faglioni, F.; Ligabue, A.; Pelloni, S.; Soncini, A.; Viglione, R. G.; Ferraro, M. B.; Zanasi, R.; Lazzeretti, P. *Org. Lett.* **2005**, *7*, 3457. (b) Stanger, A. *J. Org. Chem.* **2006**, *71*, 883.

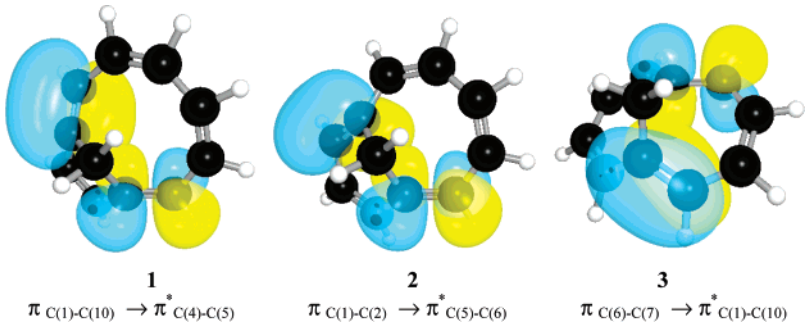

FIGURE 2. Interactions between NBOs that describe homoaromaticity.

TABLE 12. Natural Steric Analysis for the Main Resonance Structures of 1−3

	dE (kcal/mol)		
interactions[a]	**1**	**2**	**3**
$\pi_{C(1)-C(2)} \leftrightarrow \pi_{C(5)-C(6)}$		**2.47**	
$\pi_{C(1)-C(10)} \leftrightarrow \pi_{C(2)-C(3)}$	13.46		9.66
$\pi_{C(1)-C(10)} \leftrightarrow \pi_{C(4)-C(5)}$	**1.04**		
$\pi_{C(1)-C(10)} \leftrightarrow \pi_{C(6)-C(7)}$			**5.35**
$\pi_{C(2)-C(3)} \leftrightarrow \pi_{C(4)-C(5)}$	12.94		8.10
$\pi_{C(3)-C(4)} \leftrightarrow \pi_{C(5)-C(6)}$		10.83	
$\pi_{C(6)-C(7)} \leftrightarrow \pi_{C(8)-C(9)}$	8.65		6.82
$\pi_{C(7)-C(8)} \leftrightarrow \pi_{C(9)-C(10)}$		8.65	
$\pi_{C(8)-C(9)} \leftrightarrow \pi_{C(1)-C(10)}$	8.08		6.73
$\pi_{C(9)-C(10)} \leftrightarrow \pi_{C(1)-C(2)}$		9.68	
$\sigma_{C(1)-C(11)} \leftrightarrow \sigma_{C(2)-C(3)}$	10.13	6.28	
$\sigma_{C(11)-H(12)} \leftrightarrow \pi_{C(7)-C(8)}$		1.81	
$\sigma_{C(11)-H(12)} \leftrightarrow \pi_{C(8)-C(9)}$	1.96		
$\sigma_{C(11)-H(12)} \leftrightarrow \pi_{C(9)-C(10)}$		1.51	
$\sigma_{C(11)-H(12)} \leftrightarrow \sigma_{C(5)-C(6)}$		3.23	
$\sigma_{C(11)-H(12)} \leftrightarrow \sigma_{C(6)-C(7)}$	2.16		3.01
$\sigma_{C(11)-H(12)} \leftrightarrow \sigma_{C(7)-C(8)}$	3.06		0.93
$\sigma_{C(11)-H(12)} \leftrightarrow \sigma_{C(8)-C(9)}$		1.88	1.04

[a] The notation a ↔ b indicates a repulsive interaction between NLMOs a and b.

to the interference of σ framework of the methano bridges for NICS(1) and to ring carbons and hydrogens for NICS(−1).[30,45]

3.4.4. Resonance Energy. The resonance energy, RE, is an extra stability of a conjugated system as compared to that with the same number of isolated π-bonds (e.g., benzene as compared to cyclohexatriene).[31] Haddon and Fukunaga showed that the resonance energies, RE, are directly related to the HOMO−LUMO gaps in [4n + 2] annulenes, through the equation:[46]

$$\mathrm{RE} = -\frac{(\pi P_{rs})^2 \Delta E_g}{24} \qquad (1)$$

where P_{rs} is the mean value of C−C unsaturated ring natural bond orders, obtained by the NRT method, and ΔE_g is the HOMO−LUMO gap. Aside from that, this equation indicates the connection between the thermodynamic and kinetic criterion of the aromatic character. Indeed, the HOMO−LUMO gap (ΔE_g) does provide a measure of chemical stability and reactivity (stable compounds have large ΔE_g values, whereas reactive have small values). In addition, some studies have shown that a small HOMO−LUMO gap is associated with antiaromaticity.[47] The RE was determined for annulenes **1**−**3** and for **4**, because **4** has the same number of π electrons as the methano annulenes and therefore can be used as a reference compound to evaluate changes of RE for **1**−**3**.

According to Table 8, ΔE_g determines the increase of RE from **1** to **4**, because P_{rs} is larger for **2** and present a small variation for the other compounds. Consequently, the order of the aromatic stabilization decreases from **3** to **1**. It can also be observed that **4** has larger ΔE_g and RE than **3**, indicating that the bending of the annulene ring decreases the resonance. By comparing the three global aromaticity indexes, HOMA, χ_M, and RE (Tables 5, 6, and 8), we find that **1** is much less aromatic than **2** and **3**, but according to χ_M and RE, **3** is more aromatic than **2**, whereas the opposite is predicted using the HOMA index. Apart from the fact that aromaticity is a multidimensional phenomenon, and each of these indexes measures different aspects of the aromaticity, it is possible to conclude that **2** and **3** are strongly aromatic, and **1** has only a small aromaticity. It is interesting to note that the energetic stabilization obtained by homodesmotic reactions (Table 3) agrees with these aromatic indexes.

3.5. Resonance Structures − NRT Method. Resonance structures (RS) were obtained by the NRT method, and the structures with the highest weight are presented in Table 9. Compounds **2** and **3** present two RS values of equal weight, which is typical for aromatic compounds. In contrast, **1** presents a dipolar RS that has a weight 4 times lower than that of the main RS. This indicates that the resonance in the annulene ring for **1** is not so high, or this compound presents a small aromaticity. This analysis agrees with global HOMA, χ_M, and RE, indicating that **2** and **3** are more aromatic than **1**. It is interesting to note that the NRT method does not predict the existence of homoconjugation, because no RS is observed that presents a bond between bridgehead carbons. This is in contrast with valence bond calculations for **3**.[12] By using the two highest RS obtained by NRT and another one that has a bond between bridgehead carbons, it was observed that the last was more stable than the formers, indicating that this molecule is homoaromatic, according to experimental evidence.[48] Aside from that, comparing the naphthalene resonance structures weights acquired through NRT with those obtained by using VB, an opposite tendency can be observed. According to NRT results, the main resonance structure of naphthalene is **4A** (Table 9), which is degenerated. On the other hand, different VB results show that the most important contributing resonance structure is that with

(46) Haddon, R. C.; Fukunaga, T. *Tetrahedron Lett.* **1980**, *21*, 1191.

(47) (a) Dewar, M. J. S. *Angew. Chem., Int. Ed. Engl.* **1971**, *10*, 761. (b) Cava, M. P.; Mitchell, M. J. *Cyclobutadiene and Related Compounds*; Academic: New York, 1967. (c) Cohen, Y.; Roelofs, N. H.; Reinhardt, G.; Scott, L. T.; Rabinovitz, M. *J. Org. Chem.* **1987**, *52*, 4207. (d) Budzelaar, P. H. M.; Cremer, D.; Wallasch, M.; Wurthwein, E. U.; Schleyer, P. v. R. *J. Am. Chem. Soc.* **1987**, *109*, 6290.

(48) Garrat, P. J. *Aromaticity*; Wiley: New York, 1986.

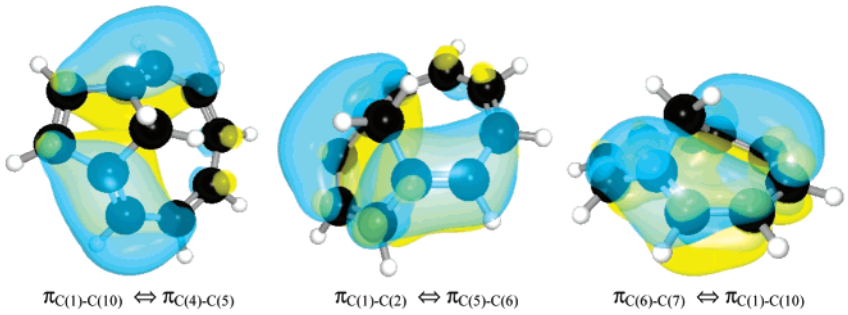

FIGURE 3. Interactions between NLMOs of **1**, **2**, and **3**.

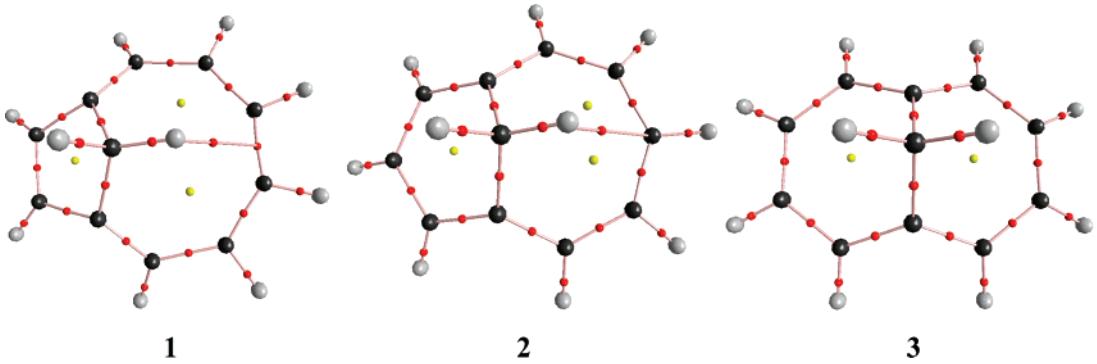

FIGURE 4. Molecular graphs of **1**, **2**, and **3**.

the maximum number of 6π-electron conjugated circuits, **4B** (Table 9).[49,50]

3.6. Attractive Interactions between Natural Bond Orbitals. NBO analysis was performed for the main RS obtained through the NRT method. The largest second-order interaction energies ($\Delta E^{(2)}$) were observed between π and π^* NBOs (Table 10). The magnitude of these interactions varies according to the difference of electron delocalization. Annulene **1** presents alternated bond lengths (Table 1), and the $\pi \rightarrow \pi^*$ interactions range between 11 and 17 kcal mol^{-1}. On the other hand, for **2** and **3** this range is 17−24 kcal mol^{-1}. As these interactions describe the π-electron delocalization, they can be related qualitatively to aromaticity. It is also possible to observe some small through-space stabilizing interactions between pure π and π^* orbitals of bridgehead carbons, characteristic of the occurrence of transanular homoconjugation,[16,51] as classified by Masamune and co-workers.[52] For this reason, **2** and **3** are referred to as homoazulene and homonaphthalene, respectively.[16] These interactions are presented in Table 11, and some are shown in Figure 2. Furthermore, we can assert that these interactions do not depend on the distance between the bridgehead carbons, because the distances of **1** and **3** are quite similar, around 2.28 Å, but the values of $\Delta E^{(2)}$ for **1** and **3** are 0.52 and 3.40 kcal mol^{-1}, respectively. For **2**, $\Delta E^{(2)}$ is 1.40 kcal mol^{-1}, and C1−C5 distance is 2.376 Å. These differences in $\Delta E^{(2)}$ can be explained by variations in the off-diagonal NBO Fock matrix element, F_{ij}, as the differences in the energies of donor and acceptor NBOs, $\epsilon_i - \epsilon_j$, are constant (Table 11). This can be attributed to changes in overlap of the orbitals involved in the transanular interactions, as F_{ij} is proportional to S_{ij} in qualitative molecular orbital theories[53] (Figure 2).

3.7. Repulsive Interactions − Natural Steric Analysis. Not only the stabilizing interactions involving NBOs, but also the steric exchange interactions between occupied disjoint (orbitals that share no common atom) NLMOs (natural localized molecular orbitals) were obtained to determine the main steric interactions that destabilize the considered annulenes. In addition, the mechanisms of occurrence of these interactions were also analyzed. In this section, these kinds of interactions are evaluated through the NSA analysis.

The largest repulsive interactions occur between adjacent π orbitals. One of them contains a π orbital of the bridgehead carbon (Table 12). This indicates that the distortion of the ring, created by the bridge, increases the overlap between occupied π orbitals, decreasing the stability of these annulenes. The largest of these interactions in **1** or **2** includes one orbital situated in ring (a), suggesting that smaller bond angles than the trigonal lead to an increase of overlap between π occupied orbitals. **1** and **2** present also a σ interaction between the C−C bond in the bridge and a C−C bond in ring (a), indicating again that the distortion in bond angles helps repulsive interactions. The largest repulsive interactions are observed for **1**, followed by **2** and **3**. This parallels the stability order, suggesting that they contribute to the instability of **1**. Other interactions can be observed between the C−H bonds of bridges and the σ and π framework of the bicyclo. Despite the small magnitude of these interactions (1.0−3.0 kcal mol^{-1}), they occur in a considerable number, indicating again that the bridges destabilize the aromatic rings.

(49) Graovac, A.; Gutman, I.; Randić, M.; Trinajstić, N. *J. Am. Chem. Soc.* **1973**, *95*, 6267.
(50) Havenith, R. W. A.; van Lenthe, J. H.; Jenneskens, L. W. *J. Org. Chem.* **2005**, *70*, 4484.
(51) Okazaki, T.; Galembeck, S. E.; Laali, K. K. *J. Org. Chem.* **2002**, *67*, 8721.
(52) Masamune, S.; Brooks, D. W.; Morio, K.; Sobezak, R. L. *J. Am. Chem. Soc.* **1976**, *98*, 8277.
(53) Rauk, A. *Orbital Interaction Theory of Organic Chemistry*; John Wiley & Sons, Inc.: New York, 1994.

TABLE 13. Properties of BCPs and RCPs (au)

		compounds		
critical points	properties	**1**	**2**	**3**
	BCPs (a)[a]			
C(1)−C(2)	ρ_b	0.278	0.300	0.299
	$-\nabla^2\rho_b$	−0.700	−0.814	−0.819
	ϵ_b	0.370	0.406	0.403
C(2)−C(3)	ρ_b	0.310	0.292	0.304
	$-\nabla^2\rho_b$	−0.841	−0.765	−0.827
	ϵ_b	0.425	0.398	0.415
C(3)−C(4)	ρ_b	0.278	0.293	0.287
	$-\nabla^2\rho_b$	−0.701	−0.766	−0.748
	ϵ_b	0.370	0.399	0.388
C(4)−C(5)	ρ_b		0.301	0.304
	$-\nabla^2\rho_b$		−0.816	−0.827
	ϵ_b		0.407	0.415
	BCPs (b)			
C(4)−C(5)	ρ_b	0.324		
	$-\nabla^2\rho_b$	−0.939		
	ϵ_b	0.443		
C(5)−C(6)	ρ_b	0.280	0.307	
	$-\nabla^2\rho_b$	−0.725	−0.861	
	ϵ_b	0.377	0.413	
C(6)−C(7)	ρ_b	0.303	0.297	0.299
	$-\nabla^2\rho_b$	−0.812	−0.802	−0.819
	ϵ_b	0.415	0.404	0.403
C(7)−C(8)	ρ_b	0.267	0.289	0.304
	$-\nabla^2\rho_b$	−0.649	−0.755	−0.827
	ϵ_b	0.359	0.393	0.415
C(8)−C(9)	ρ_b	0.303	0.289	0.287
	$-\nabla^2\rho_b$	−0.811	−0.752	−0.748
	ϵ_b	0.415	0.392	0.388
RCP (a)	ρ_b	0.050	0.024	0.013
	$-\nabla^2\rho_b$	0.304	0.167	0.082
	ϵ_b	0.058	0.016	0.003
RCP (b)	ρ_b	0.014	0.014	0.013
	$-\nabla^2\rho_b$	0.064	0.061	0.082
	ϵ_b	0.010	0.008	0.003
C(1)−C(11)	ρ_b	0.256	0.256	0.256
	$-\nabla^2\rho_b$	−0.618	−0.614	−0.612
	ϵ_b	0.331	0.331	0.334

[a] The indexes (a) and (b) refer to the CPs from ring fragments (a) and (b).

Some destabilizing interactions (in bold type) between π orbitals that contain the bridgehead carbon atoms are observed, which are similar to the stabilizing interactions between NBOs that describes homoaromaticity (Figure 3). It is interesting to note that the energy of these interactions increases from **1** to **3**, which indicates that there is no correlation between bridgehead carbons distances and this energy. The same is observed for homoconjugated interaction between NBOs. The order of steric energy is determined by the overlap integral between NLMOs.

3.8. Topology of the Electron Density. Figure 4 shows the molecular graphics of **1**−**3** obtained by AIM analysis, where the atoms are indicated by spheres, the bond critical points (BCPs) by red, and the ring critical points (RCPs) by yellow dots. The topologies are consistent with the Poincaré−Hopf relationship.

Table 13 presents some parameters for the critical points. The differences between the electron densities for the formally single and double bonds are larger for **1** than for **2** and **3**, indicating an increase in delocalization of π electrons. The same behavior is observed for the Laplacian of the electron density ($\nabla^2\rho_b$) and for the ellipticity (ϵ_b). These results correlate with HOMA, NICS, RE, NBO, and NSA analysis. It is also interesting to note that the critical point properties for the C−C bond in the bridge are not affected by changes in the rings, as observed for bond lengths (Table 2). With respect to the RCPs of **1** and **2**, located in ring (b) (RCP (b)), only one is presented in Table 13 because they are related by symmetry.

The molecular graphics for **1** present a bond path between a hydrogen of the bridge, H(12), and the carbon−carbon BCP in the ring, C(7)−C(8) (Figures 1 and 4). This indicates that a conflict mechanism is occurring. This conflict structure is energetically and topologically unstable, which means that a slight conformational change will modify the distance between the hydrogen atom and the CC bond, and, therefore, the BCP will vanish.[26] For **2**, a bond path connects a hydrogen atom of the bridge, H(12), with a carbon ring atom, C(8). The presence of these two bond paths can be partially attributed to the proximity between H(12) and C(8), as the distance H(12)−C(8) is similar for **1** and **2** (4.4 and 4.6 Å, respectively), but for **3** this distance is 5.1 Å. To characterize the nature of these interactions, a similar procedure, as reported by Matta and co-workers about the hydrogen−hydrogen interactions in polybenzenoids, was employed.[54] The parameters of these BCPs (ζ_1 and ζ_2) were determined and compared to BCPs of ordinary C−C bonds (Table 14. The results indicate that both interactions exhibit characteristics of closed-shell interactions:[55] a low value for the density ρ_b, a relatively small positive value for $\nabla^2\rho_b$, and positive values of $H(r)$ at ζ. The bond path length (BPL) is curved and exceeds the bond lengths (BL). In addition, the ellipticity, ϵ, values at ζ are very large in comparison with the ellipticity at BCP_{ring}, indicating instability. Despite the fact that the distances between BCPs and RCPs ($r_b - r_r$) are small, the difference between these densities ($\rho_b - \rho_r$) is approximately zero at ζ_1 and ζ_2. Therefore, according to the above-mentioned parameters, these interactions are topologically unstable, indicating that a small change in the molecular geometry will produce a collapse between the BCP and RCP. There is a strong debate in literature if nonbonded steric interactions are attractive or repulsive. Bader and co-workers pointed out that the occurrence of a bond path indicates a stabilizing interaction.[54,56] Several authors do not agree with this view and demonstrate that steric interactions are repulsive using the AIM method or other techniques.[57,58] As indicated by NSA analysis, the interaction between σ(C−H) orbitals in the bridge and π or σ orbitals in the ring is repulsive, and so the existence of a nonbonded bond paths in **1** and **2** should not indicate an stabilizing interaction. It is interesting to note that there is no BCP between the atoms involved in the homoconjugated interaction, despite the large experimental indication for the homoaromaticity of these compounds.[59,60] A common observation is that AIM does not indicate the existence of homoconjugative interaction, even in systems with clear experimental evidence, as in the homocyclopropenyl cation.[61−63]

(54) Matta, C. F.; Trujillo, J. H.; Tang, T. H.; Bader, R. F. W. *Chem.-Eur. J.* **2003**, *9*, 1940.
(55) Cremer, D.; Kraka, E. *Angew. Chem., Int. Ed. Engl.* **1984**, *23*, 627.
(56) Bader, R. F. W. *Chem.-Eur. J.* **2006**, *12*, 2896.
(57) (a) Cioslowski, J.; Mixon, S. T. *Can. J. Chem.* **1992**, *70*, 443. (b) Cioslowski, J.; Mixon, S. T. *J. Am. Chem. Soc.* **1992**, *114*, 4382.
(58) (a) Haaland, A.; Shorokhov, D. J.; Tverdova, N. V. *Chem.-Eur. J.* **2004**, *10*, 4416. (b) Poater, J.; Solà, M.; Bickelhaupt, F. M. *Chem.-Eur. J.* **2006**, *12*, 2889. (c) Poater, J.; Solà, M.; Bickelhaupt, F. M. *Chem.-Eur. J.* **2006**, *12*, 2902.
(59) Dewey, H. J.; Deger, H.; Frölich, W.; Dick, B.; Klingensmith, K. A.; Hohlneicher, G.; Vogel, E.; Michl, J. *J. Am. Chem. Soc.* **1980**, *102*, 6412.
(60) Scott, L. T. *Pure Appl. Chem.* **1986**, *58*, 105.

TABLE 14. Bond Critical Point Parameters in au

compounds	CPs	ρ_b	$-^2\rho_b$	ϵ	G_b	V_b	H_b	$r_b - r_r$	$\rho_r - \rho_b$	BL	BPL
1	ζ_1	0.016	0.064	6.960	0.014	0.011	0.003	1.772	0.002	4.142	5.494
	BCP_{ring}	0.278	0.700	0.149	0.091	0.358	0.266	1.872	0.228	2.734	2.736
2	ζ_2	0.014	0.055	3.186	0.012	0.009	0.007	0.928	0.000	4.643	4.816
	BCP_{ring}	0.292	0.765	0.398	0.105	0.401	0.296	2.241	0.268	2.669	2.670

TABLE 15. B3LYP/6-31G* Average Bond Orders *K* (Plain Numbers) and Standard Deviation (in Italics) for Molecules 1−3 and Their Composing Fragments

compounds	K	K_a	K_b
1	1.462	1.318	1.462
	0.213	*0.232*	*0.207*
2	1.413	1.392	1.419
	0.019	*0.018*	*0.009*
3	1.412	1.403	1.407
	0.089	*0.085*	*0.085*

3.9. Generalized Population Analysis. Ponec, Bultinck, and co-workers[27,64] have recently introduced the use of generalized population analysis (GPA) as a new aromaticity criterion following the earlier suggestion by Giambiagi[65] et al. in a slightly different scheme. It has been shown that GPA can be used for many different cases of aromaticity, including heteronuclear homoaromaticity. GPA provides *n*-center bonding $P_{AB...N}$ indices between atoms A,B,...N via the generic equation:

$$P_{AB...N} = \alpha \sum_{\nu \in A} \sum_{\mu \in B} ... \sum_{\sigma \in N} \sum_{i} \Gamma_i[(PS)_{\nu\mu}(PS)_{\mu x}...(PS)_{\sigma\nu}] \qquad (2)$$

P and *S* are respectively the density matrix and the overlap matrix, and the notation $\nu \in A$ means that a summation should be carried out over all basis functions $\nu \in A$ centered on A. The operator Γ_i is a permutation operator designed at generating all necessary $(n - 1)!$ terms in the expression for $P_{AB...N}$, and α is a theoretically derived constant. It is immediately clear that in the case of just a 2-center bond, these bond indices are equal to the Wiberg bond order, later generalized to the non-orthogonal case by Giambiagi et al. and later Mayer.[66]

The deviation from equality between the different diatomic bond orders between adjacent atoms in the annulene ring can be used as a first indication of the change in aromaticity. Table 15 gives the average bond order between all carbon atom pairs in the annulene ring, with the standard deviation as a measure of the spread among the individual values.

Table 15 reveals that **2** is the ring with the most equalized bond orders, followed by **3** and ultimately **1**. From the values in Table 13, we see that the values for *K* yield to the same conclusion as the HOMA values in Table 5. Consistent with the smallest variation in bond lengths, the standard variation on the bond orders is also the smallest in compound **2**.

TABLE 16. B3LYP/6-31G* Multicenter Bond Orders for Both Possibly Homoaromatic Rings in Molecules 1−3 (P_a and P_b)

compounds	P_a	P_b
1	−0.0150	−0.0091
2	0.0130	0.0020
3	0.0180	0.0180

One could hypothesize the presence of homoaromaticity in the fragments of the annulene rings. To examine the presence of homoaromaticity, we computed the corresponding GPA indices for the homoaromatic rings that could possibly be formed. For each of the possible subrings in the different molecules, the multicenter index was computed. The results for all rings are shown in Table 16.

Especially the 1,6-methano[10]annulene, **3**, is an interesting case. It is commonly known that the six-membered subrings are homoaromatic.[67] The so-called six center index (SCI, the specific case for a six-membered ring)[64] for this molecule in Table 16 nicely illustrates this. The value of 0.019 is of nearly the same magnitude as for the six-membered rings in anthracene and only slightly lower than for the six-membered rings in naphthalene (0.026). The case of six-membered rings is the best studied, and the SCI results are confirmed by other electron delocalization indices, such as the para delocalization index (PDI) and the fluctuation index (FLU) introduced by Solà and co-workers.[68] The values for both latter indices computed in a Mulliken approach are respectively 0.059 and 0.141, again very similar to the naphthalene six-membered rings.

One of the nice features of the multicenter indices is that they can be extended easily to rings of any size and do not require some reference value. Table 16 therefore also reports values for the multicenter indices for the other rings. Considering the fact that the indices always grow smaller with increasing size of the delocalized system, one sees immediately that the six-membered rings in **3** are certainly the most homoaromatic.

As a conclusion, we find that, for the smaller rings, homoaromaticity plays the most important role in rings (a) and (b) of **3**, and in the other molecules homoaromaticity is much less important.

4. Conclusions

The electronic structure, aromaticity, and homoaromaticity of three bridged methano[10]annulenes were studied. The geometrical parameters pointed out that the bond lengths of **1** are more alternate than the bond lengths of **2** and **3**, presenting a close agreement with aromatic indexes. In addition, the planarity of the rings, estimated through the dihedral angles on the neighborhood of the methano bridges, showed the order **3** > **2** > **1**, which is related to the increase of the aromaticity.

(61) Cremer, D.; Kraka, E.; Slee, T. S.; Bader, R. F. W.; Lau, C. D. H.; Nguyen-Dang, T. T.; MacDougall, P. J. *J. Am. Chem. Soc.* **1983**, *105*, 5069.
(62) Werstiuk, N. H.; Muchall, H. M. *J. Mol. Struct. (THEOCHEM)* **1999**, *463*, 225−229.
(63) (a) Werstiuk, N. H.; Muchall, H. M. *J. Phys. Chem. A* **2000**, *104*, 2054. (b) Werstiuk, N. H.; Muchall, H. M.; Noury, S. *J. Phys. Chem. A* **2000**, *104*, 11601.
(64) Bultinck, P.; Ponec, R.; Van Damme, S. *J. Phys. Org. Chem.* **2005**, *18*, 706.
(65) Giambiagi, M.; Giambiagi, M. S.; Mundim, K. C. *Struct. Chem.* **1990**, *1*, 423.
(66) (a) Wiberg, K. *Tetrahedron* **1968**, *24*, 1083. (b) Giambiagi, M.; de Giambiagi, M. S.; Grempel, D. R.; Heymann, C. D. *J. Chim. Phys.* **1975**, *72*, 15. (c) Mayer, I. *Chem. Phys. Lett.* **1983**, *97*, 270.
(67) Clayden, J. P.; Greeves, N.; Warren S.; Wothers, P. D. *Organic Chemistry*; Oxford University Press: Oxford, UK, 2001.
(68) (a) Poater, J.; Fradera, X.; Duran, M.; Solà, M. *Chem.-Eur. J.* **2003**, *9*, 400. (b) Matito, E.; Duran, M.; Solà, M. *J. Chem. Phys.* **2005**, *122*, 014109-1.

The homodesmotic reactions SE(HD) showed that **1** is the most strained isomer, **2** presents an intermediate strain, and **3** is the least strained isomer. The partitioning of the strain energies indicated that the rings of **1** and **2** absorb more tension than the ring of **3**. On the other hand, the bridge of **3** is the most strained. All global indexes of aromaticity, global HOMA, RE, and χ_M, indicated that **1** is fairly aromatic, in contrast to **2** and **3**. This agrees with the order of aromatic stabilization, as calculated by homodesmotic reactions. It is interesting to note that both HOMA and GPA describe that **2** has more aromatic stabilization than **3**. The NBO method presented some interactions involving orbitals of bridgehead carbons that can suggest the existence of homoaromaticity. On the other hand, AIM theory pointed out that the considered annulenes do not present stabilization by homoaromaticity, in disagreement with experimental data. GPA points out that homoaromaticity plays a relevant role only in **3**.

Acknowledgment. We acknowledge the Brazilian foundations FAPESP, CAPES, and CNPq for financial support. K.T.O. and G.F.C. thank FAPESP for Ph.D. scholarships (Grants 01/11204-9 and 02/03753-5, respectively), and S.E.G. thanks CNPq for a research scholarship (Grant 452292/2005-0).

Supporting Information Available: Total energies and the number of imaginary frequencies (Table S1), and the Cartesian coordinates of the optimized geometries of **1**, **2**, **3**, and **4** (Tables S2−S5). This material is available free of charge via the Internet at http://pubs.acs.org.

JO061702V